Optica Applicata, Vol. XL, No. 3, 2010

A multimode interference polymer-silica hybrid waveguide 2×2 thermo-optic switch

X.Q. SUN, C.M. CHEN, F. WANG, J. SUN, W.N. GAO, L. GAO,
H.L. ZHENG, C.P. KANG, D.M. ZHANG*

State Key Laboratory on Integrated Optoelectronics, College of Electronic Science and Engineering, Jilin University, Changchun 130012, P.R. China

*Corresponding author: zhangdm@jlu.edu.cn

A polymer-silica hybrid 2×2 thermo-optic switch is demonstrated. The top cladding and core layer are composed of polymers, while the bottom cladding is made of silica. Since polymer and silica have opposite signs of thermo-optic coefficients, the change of the refractive index of the core is opposite to that of the bottom cladding as the temperature increased. With the finite difference beam propagation method (FD-BPM) and thermal coupling simulation, the proposed device presents a crosstalk of 20 and 18 dB at bar state and cross state, respectively. The device also exhibits extinction ratios of 19 and 27 dB at each state. In addition, the low absorption of material and simple structure of the device enable the insertion loss to be 17 dB. Also the electrical power consumption is about 45 mW at $\lambda = 1.55$ μm. The rise time and fall time of switching are 0.2 ms and 0.4 ms, respectively.

Keywords: polymer waveguide device, thermo-optic effects, optical switches.

1. Introduction

Optical switches are essential components in optical cross connecting protection switching, optical signal monitoring and optical add/drop multiplexing (OADM). Different approaches have been investigated to improve the performance, such as utilizing the electro-optic (EO) effect to realize fast optical switches [1, 2]. But these approaches either suffer from complicated techniques, or from high fabrication cost and inconvenience for integration. Because the large thermo-optic (TO) coefficients and low thermal conductivity can result in effective modulation, polymer optical switches based on TO effect become a promising method for integrating multi-functional devices and mass production with low cost [3, 4]. It is especially favorable to employ silicon as the substrate which would serve as a good heat sink. Due to different thermal characteristics of polymers and silicon, stress is induced in the waveguide films [5]. Therefore, integrating the above features into hybrid TO switches has been reported [6].

Different types of optical waveguide switches have been fabricated, including directional coupler, Y branch and multimode interference (MMI). The directional coupler switch is very sensitive to dimension size in the processing of fabrication. Though the Y branch switch is independent of polarization in a certain range of wavelength, it needs larger length to obtain suitable operating voltage and requires more electrical power to achieve low crosstalk. As to MMI coupler, it shows good features of compactness, suitability for integration and fabrication tolerances compared to the above switches [7].

In this paper, we demonstrate a novel MMI waveguide thermo-optic switch, of which one heating electrode is used for switching operation [8]. Compared to the previous polymer thermo-optic switch, in which SiO_2 is adopted as the bottom cladding of the waveguide, the electrode structure is optimized to reduce the electrical power consumption.

2. Configuration and principle

In this paper, the proposed TO switch is based on MMI effect. The schematic diagram of the device is shown in Fig. 1. It consists of two couples of input/output waveguides and a channel MMI coupler, which is heated by an electrode. Different from the conventional polymer switches, the waveguide of the proposed switch consists of two different materials. The top cladding and core layer are polymer materials, while the bottom cladding is silica, which is useful to achieve faster switching speed. Since silica and polymer have opposite sign of thermo-optic coefficients, as the temperature increases, the refractive indices of the core and the bottom cladding shift reversely. The silicon substrate functions as a heat sink because of its large thermal conductivity. And for this reason, it is confirmed that the hybrid waveguide exhibits the bar state when electric power is applied.

In our design, the polymethyl methacrylate glyciclyl methacrylate (PMMA-GMA) material is adopted to fabricate the device, which is low cost and easy fabrication.

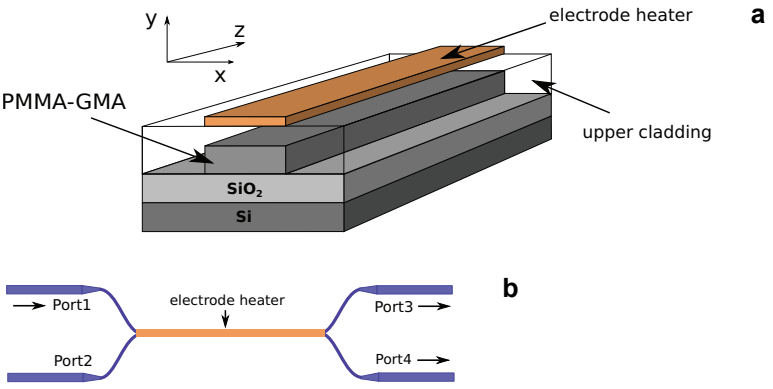

Fig. 1. Schematic diagram and cross-section view of MMI optical switch.

T a b l e. Thermal parameters and refractive indices used in the simulation.

Material	Thermal conductivity [$W m^{-1} °C^{-1}$]	Thermo-optic coefficient [$°C^{-1}$]	Refractive index	Position
Al	407	–	–	Heating electrodes
PMMA-GMA (bis-A-epoxy)	0.2	-1.2×10^{-4}	1.492	Core
PMMA-GMA	0.2	-1.2×10^{-4}	1.483	Top cladding
SiO_2	1.4	10×10^{-4}	1.45	Lower cladding

The structure includes a 4 μm thick core layer of PMMA-GMA with bis-A-epoxy, of which the refractive index is 1.492 at 1550 nm. The PMMA-GMA is used as the upper cladding. Its refractive index is 1.483 at 1550 nm. The TO coefficient of PMMA-GMA and the lower cladding SiO_2 is -1.2×10^{-4} $°C^{-1}$ and $+1\times10^{-5}$ $°C^{-1}$, respectively.

In order to determine the geometrical size of the proposed switch, numerical calculations are carried out [9], based on the following MMI imaging formula:

$$L_\pi = \frac{4 n_f W_{\mathrm{MMI}}^2}{3\lambda_0} \tag{1}$$

where we take the effective refractive index n_f as 1.486, the width of MMI waveguide W_{MMI} as 12 μm, and the operation wavelength λ_0 as 1.55 μm. Then the characteristic imaging length is calculated to be 184 μm.

For our case, the optical and thermal behaviors of the device are analyzed by Beam PROP^{TM}, which is based on the finite difference beam propagation method (FD-BPM) [10]. The software could be applied to confirm the fluctuation of the refractive index in the waveguide. In this work, design optimization is performed for coupling rectangle waveguide and SMF-28 fiber, the geometrical size of S-bend waveguide, the MMI waveguide and the heating electrodes length. The thermal parameters and refractive indices are listed in the Table, which are used in the following simulation [11].

Figure 2 shows the optical power distributions of the light at the cross state and the bar state. The facet of the input S-bend and the MMI coupler is located at the position of $Z = 0$. The heating electrode is placed on the top cladding along the MMI waveguide. As to the MMI waveguide size, increasing the width of MMI coupler is undesirable in the application, because it would lengthen the device remarkably. Increasing the thickness of the MMI waveguide can improve self-imaging quality and uniformity, so this technique will become the best choice [12].

In this design, the input/output waveguide widths at the interface of the fiber and the device are chosen to be 8 μm, because the mode field diameter of the single mode fiber SMF-28 is 8 μm – 10 μm, and enlarging the waveguide width can improve the mode size matching and reduce the coupling loss effectively. Since the width of MMI is 12 μm, we adopt S-bend and tapered waveguides which change the waveguide

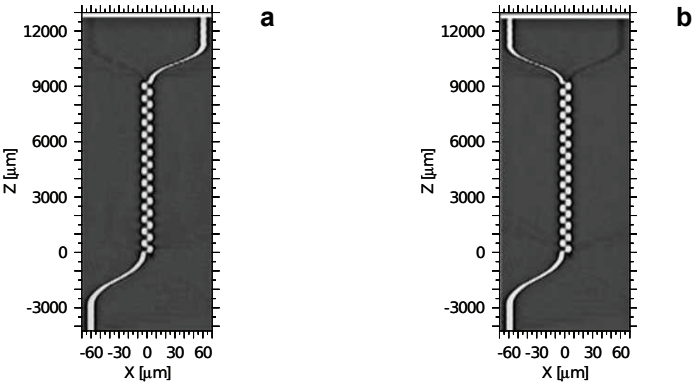

Fig. 2. Beam propagation calculation of the polymer-silica hybrid waveguide structure. Current = 0 mA (**a**), Current = 3.2 mA (**b**).

width gradually from 8 μm at the position of the input ports to 4 μm at the position of $Z = 0$. And waveguide width changes from 4 μm at the position of $Z = 9312$ μm to the output ports gradually, which is shown in Fig. 2 [11, 13].

According to the above analysis and simulation, the MMI waveguide size was determined to be 12 μm×4 μm at 1550 nm with an index contrast of 0.6% and the length of the MMI coupler was chosen to be 9312 μm. 3 μm thick SiO_2 and 6 μm thick PMMA are adopted as the bottom cladding and top cladding, respectively. The two input/output waveguides in S-bend were positioned at 1/3 and 2/3 of the whole MMI coupler width.

The temperature distribution inside the waveguide layers due to the constant temperature elements is determined by solving Poisson's equation [14]:

$$-\nabla\left[K(x, y, z)\nabla T(x, y, z)\right] = Q(x, y, z) \tag{2}$$

where $T(x, y, z)$ is the temperature and $Q(x, y, z)$ is the heat generated per unit volume within the waveguide layers.

From the above analysis, in the absence of applied power, light coupled to port 1 is emitted from port 4, and vice-versa. However, when a π phase shift is applied to the self-image, the light coupled to port 1 will be imaged onto port 3 as shown in Fig. 2. The phase shift is controlled by the following equation:

$$\Delta\phi = k\Delta n L_h \tag{3}$$

where $k = 2\pi/\lambda$, the phase shift is induced by the change of the refractive index n along the tunable section with the heater length L_h for a signal at $\lambda = 1.55$ μm. The change of refractive index $\mathrm{d}n/\mathrm{d}T$ is dependent on the TO coefficient of material and change of temperature ΔT [13]

$$\Delta n = \frac{\mathrm{d}n}{\mathrm{d}T}\Delta T \tag{4}$$

The TO coefficient of the PMMA is -1.2×10^{-4} °C^{-1}, from Eqs. (3) and (4), the relative temperature increase in our design is

$$\Delta T = \frac{1.55 \times 10^4}{2.4 L_h} \tag{5}$$

According to the calculation, when the coupling length is about 9312 μm, ΔT is about 0.7 °C. Since the heating electrode is on the surface of the top cladding, the temperature in the top cladding is larger than that in the core waveguide, and smaller than that in the bottom cladding SiO_2. The perturbation could be described by the following heat transfer Fourier's equation in transient condition with constant thermal conductivity [15]

$$\rho c_p \frac{\partial T}{\partial t} = K \nabla^2 T + Q(x, y, z, t) \tag{6}$$

where ρ is the density of materials (kg m^{-3}), c_p is the specific heat (J kg^{-1} °C^{-1}), K is the thermal conductivity (W m^{-1} °C^{-1}), $Q(x, y, z, t)$ is the heat generation per unit volume (Wm^{-3}).

The extinction ratio and the cross talk of the conventional waveguide consisting of only polymer are compared to those of the polymer-silica hybrid waveguide in the simulation, which are shown in Figs. 3 and 4. We can see that the extinction ratio of the hybrid structure is higher than the conventional one, while the cross talk is lower than it is in both states. Curves of the conventional one are more smooth than those of the hybrid structure, which exhibits two sharp peaks in bar state.

Figure 5 shows the switching characteristics of the device. We can see that when the same electrical power is applied on the electrode, the hybrid waveguide

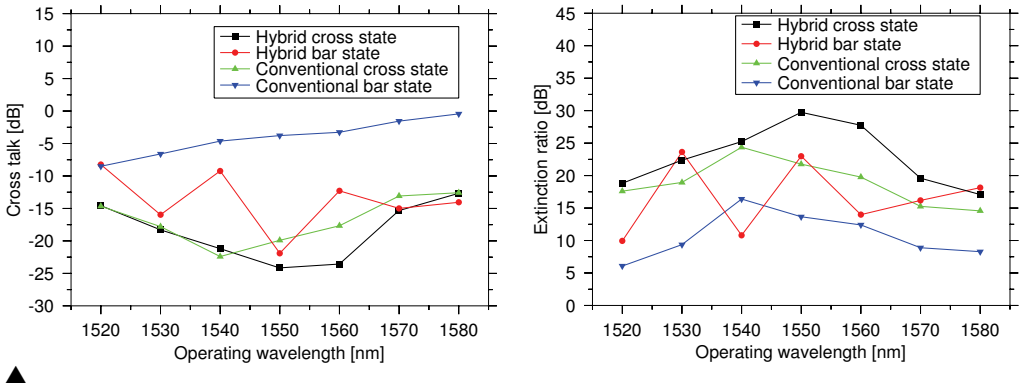

▲

Fig. 3. Simulations of spectral characteristics of cross talk at cross state and bar state for hybrid structure and conventional structure.

Fig. 4. Simulations of spectral characteristics of extinction ratio in cross state and bar state for hybrid structure and conventional structure.

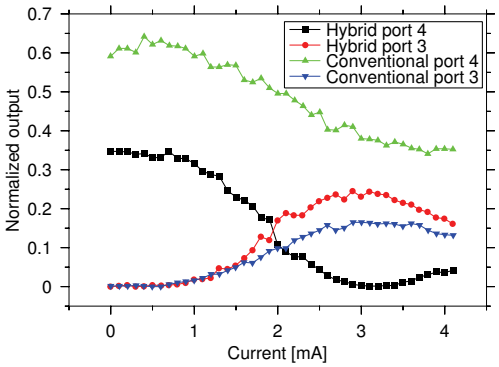

Fig. 5. Comparison of switching characteristics for hybrid and conventional structures.

structure presents better extinction ratio than the conventional one. It corresponds to the simulation above. According to the calculation, the device will exhibit switching behavior when 3.6 mW electric power is applied to the electrode [12].

3. Fabrication

The fabrication process of the proposed hybrid device is as follows: a silicon wafer was used as a substrate. The bottom cladding of a silica layer of 3 μm thick was formed on the substrate by thermal oxidation method. Polymethyl methacrylate glyciclyl methacrylate (PMMA-GMA) with bis-A-epoxy was adopted as the core layer material. It was spin coated to be 4 μm thick on the bottom cladding and was baked at 120 °C for 3 hours to remove the solvent. Then, the photoresist was spun coated on a metal mask, which was vaporized on the core layer. The photoresist was baked at 80 °C for 20 min, and exposed for 40 s under UV light (10 mW/cm^2) at the 365 nm wavelength with a photomask for wet etching. After that, reactive ion etching (RIE) was carried out in oxygen atmosphere for 40 min to form the switch pattern. Afterwards, the top cladding of 6 μm thick was formed so as to improve the efficiency of guided mode index modulation and decrease the roughness of the waveguide surface after RIE processing [16].

Finally, the electrode for thermal heating was formed by vacuum evaporation of Al on the top cladding, patterned through photolithography and wet etching. The thickness of the electrode was about 200 nm. After the device was diced, end facets of the device were polished, and the optical fibers were attached to the input and output waveguide of the device.

4. Experiments results and discussion

An important performance characteristic of an optical switch is the dependence on the wavelength. To obtain the operational characteristics of the fabricated device, the output light from a tunable semiconductor laser is launched into the input port 1. The optical power output from the port 4 and port 3 are monitored by an optical

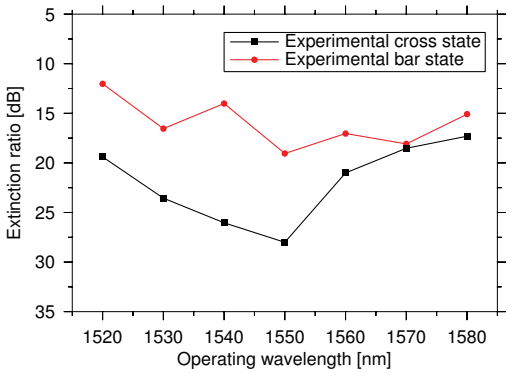

Fig. 6. Measured extinction ratio and cross talk in cross state and bar state.

spectrum analyzer [17]. With the electrode turning on and off, the spectral characteristics of the extinction ratio obtained from monitoring the two output ports are shown as curves in Fig. 6. The extinction ratio observed in bar state is higher than that in cross state, which is believed to be caused by the dimension difference between the practical situation and the design.

When the wavelength ranges from 1520 nm to 1580 nm, the cross talk experiences a large change, which is shown in Fig. 7. This renders the switch to be only suitable for working in a narrow range of wavelengths around 1550 nm.

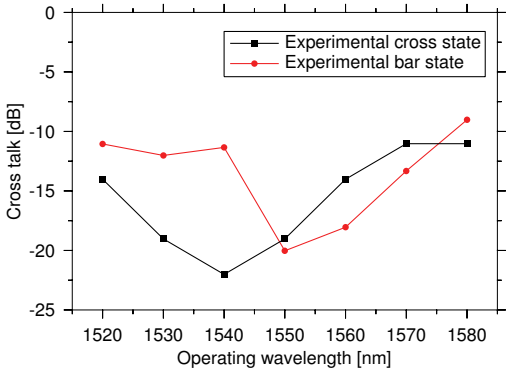

Fig. 7. Measured cross talk at cross state and bar state.

Figure 8 shows the experimental switching characteristics of this device. Because of the high contact resistance existing at the interface of the probe and the electrode, the insertion loss fluctuates in the power range. And the practical driving power is much higher than that in the simulation. If this resistance could be reduced effectively, the driving power is expected to be much smaller.

With the best alignment, the fiber-to-fiber insertion loss of a 2 cm long chip is tested to be about 17 dB at 1550 nm, of which some 10 dB is estimated to be caused by the fiber chip coupling. From the cut-back loss measurement of the straight waveguide, the propagation loss of the polymer waveguide is found to be about 2 dB/cm. The remaining 3 dB is due to the wall roughness of the waveguide and the mutual coupling between branch waveguides. It is confirmed that the initial

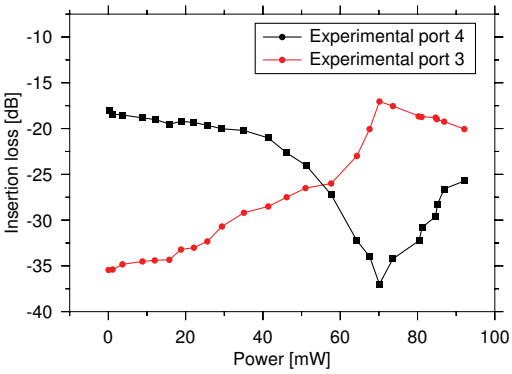

Fig. 8. Experimental switching characteristics of the device.

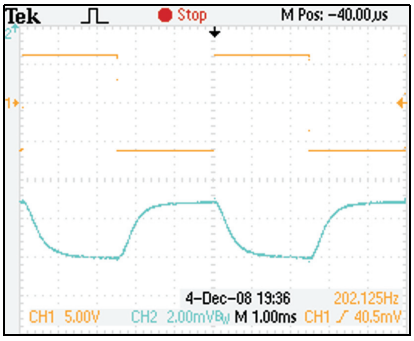

Fig. 9. Temporal switching characteristics of the device.

guided mode of the hybrid optical waveguide leaks completely to the bottom cladding with an applied electrical power of 45 mW.

Figure 9 shows the optical response of temporal switching characteristics observed by an oscilloscope. It strongly supports the validity of the switching function outlined above. Also, we can find that the rise time and the fall time of switching are 0.2 and 0.4 ms, respectively. The waveguide boundary difference between the design and the actual condition changes the temperature dispersion. That is another factor which will affect the switching speed.

5. Conclusions

A 2×2 multimode interference polymer-silica hybrid thermo-optic switch with relatively low power consumption is proposed and demonstrated experimentally. This device employs two different materials, polymer and silica, which have opposite thermo-optic coefficients. Due to the hybrid structure, the device shows relatively good compactness and high fabrication tolerance. So this 2×2 switching element is considered to be a suitable building block for constructing larger polymer-based switching matrices.

Acknowledgments – This work is supported by the National Basic Research Program of China under Grant No. 2006CB302803.

Reference

[1] ROSHAN THAPLIYA, SHIGETOSHI NAKAMURA, TAKASHI KIKUCHI, *High speed electro-optic polymeric waveguide devices with low switching voltages and thermal drift*, Proceedings of Optical Fiber Communication Conference, February 24, 2008, San Diego, California, pp. 1–3.

[2] ENAMI Y., MATHINE D., DEROSE C.T., NORWOOD R.A., LUO J., JEN A.K.-Y., PEYGHAMBARIAN N., *Hybrid cross-linkable polymer/sol–gel waveguide modulators with 0.65 V half wave voltage at 1550 nm*, Appllied Physics Letter **91**(9), 2007, p. 093505.

[3] DIEMEER M.B.J., BRONS J.J., TROMMEL E.S., *Polymeric optical waveguide switch using the thermo-optic effect*, Journal of Lightwave Technology **7**(3), 1989, pp. 449–453.

[4] CHEN R.T., *Polymer-based photonic integrated circuits*, Optics and Laser Technology **25**(6), 1993, pp. 347–365.

[5] HAUFFE R., PETERMANN K., *Thermo-Optic Switching*, 1st Edtion, Springer, US, 2006, pp. 129–133.

[6] DONG-MIN YEO, SANG-YUNG SHIN, *Polyer–silica hybrid 1×2 thermooptic switch with low crosstalk*, Optics Communications **267**(2), 2006, pp. 388–393.

[7] CHONG SIEW KUANG, SAHBUDIN SHAARI, *Polymer thermooptic switch for C-band based on multimode interference Mach–Zehnder interferometer*, Proceedings of International Symposium on Consumer Electronics, September 1–3, 2004, Reading, United Kingdom, pp. 463–467.

[8] FAN WANG, JIANYI YANG, LIMEI CHEN, XIAOQING JIANG, MINGHUA WANG, *Optical switch based on multimode interference coupler*, IEEE Photonics Technology Letters **18**(2), 2006, pp. 421–423.

[9] SOLDANO L.B., PENNINGS E.C.M., *Optical multi-mode interference devices based on self-imaging: Principles and applications*, Journal of Lightwave Technology **13**(4), 1995, pp. 615–627.

[10] ABDULAZIZ M. AL-HETAR, ABU SAHMAH M. SUPA'AT, MOHAMMAD A.B., YULIANTI I., *Crosstalk improvement of a thermo-optic polymer waveguide MZI-MMI switch*, Optics Communications **281**(23), 2008, pp. 5764–5767.

[11] CARIOU J.M., DUGAS J., MARTIN L., MICHEL P., *Refractive-index variations with temperature of PMMA and polycarbonate*, Appllied Optics **25**(3), 1986, pp. 334–336.

[12] YASUHIRO HIDA, HIDEKATSU ONOSE, SABURO IMAMURA, *Polyer waveguide thermooptic switch with low electric power consumption at 1.3 μm*, IEEE Photonics Technology Letters **5**(7), 1993, pp. 782–784.

[13] LEUTHOLD J., JOYNER C.H., *Multimode interference couplers with tunable power splitting ratios*, Journal of Lightwave Technology **19**(5), 2001, pp. 700–707.

[14] BILOTTI A.A., *Static temperature distribution in IC chips with isothermal heat sources*, IEEE Transactions on Electron Devices **21**(3), 1974, pp. 217–226.

[15] JALURIA Y., TORRANCE K.E., *Computational Heat Transfer*, 2nd Edition, Taylor and Francis, NY, 2003.

[16] ZHOU J., WONG W.H., PUN E.Y.B., SHEN Y.Q., ZHAO Y.X., *Fabrication of low loss optical waveguides with a novel thermo-optical polymer material*, Optica Applicata **36**(2–3), 2006, pp. 429–435.

[17] KAIXIN CHEN, PAK L. CHU, KIN SENG CHIANG, HAU PING CHAN, *Design and fabrication of a broad-band polymer vertically coupled optical switch*, Journal of Lightwave Technology **24**(2), 2006, pp. 904–911.

Received May 11, 2009
in revised form August 21, 2009